AIAA JOURNAL
Vol. 30, No. 3, March 1992

Streamwise Vortex Production by Pitched and Skewed Jets in a Turbulent Boundary Layer

Debora A. Compton* and James P. Johnston†
Stanford University, Stanford, California 94305

Weak longitudinal (streamwise) vortices produced by the interaction of simple, round wall jets with a two-dimensional flow comprising a turbulent boundary layer were studied experimentally. Like the jets used in the vortex generator jet (VGJ) method of stall control, the jets in this study were pitched up at 45 deg and skewed relative to the freestream as they entered from the wall. Skew angles of 90–45 deg produced the strongest vortices, and vortex strength increased with jet speed over the range studied, $VR = U_j/U_\infty = 0.7$ to 1.3. It is shown through comparison to other work that the vortices produced by the jets are similar to weak vortices produced by a solid vortex generator, but different from a strong vortex from a larger solid generator.

Nomenclature

U = mean velocity component in streamwise direction
U_j = jet speed
U_∞ = nominal freestream mean velocity
V = mean velocity component in wall-normal direction
VR = ratio, U_j/U_∞
W = mean velocity component in the spanwise direction
x = streamwise component of tunnel coordinate system, $x = 0$ at trip, Fig. 1
y = wall-normal component of tunnel coordinate system
z = spanwise component of tunnel coordinate system, $z = 0$ at surface centerline
δ_{99} = boundary-layer thickness: y location where $U = 0.99U_\infty$
θ = jet skew angle, 0 deg being downstream
Ω_x = streamwise (axial) component of mean vorticity

Introduction

JETS issuing through small holes in a flow surface (wall) have proven effective in the control of turbulent boundary-layer separation resulting from adverse pressure gradients.[1–4] The beneficial effect is obtained only if the jets are pitched and skewed with respect to the main flow direction. The interaction of the wall-jet flow with the main flow, close to the point of injection, generates a weak longitudinal vortex that persists well downstream and enhances cross-stream mixing. The technique is known as the vortex generator jet (VGJ) method of separation or stall control because it controls stall in the same general way as the well-known method using solid vortex generators.[5]

Streamwise vortices, however generated, have applications in stall control on wings and in diffusers, and in the enhancement of shear-layer mixing in dump combustors.[6] Vortices generated by VGJs, unlike those from fixed, solid, vortex generators, lend themselves to *active* control of stall, since the jet strength may be easily controlled, by valves for example. Also, for flow situations when stall control is not needed, the parasitic losses (e.g., drag) associated with solid generators are avoided with the jet flow turned off. However, rational design of practical VGJ control systems requires more basic knowledge on the flows produced by skewed and pitched wall jet. The goal of this work was to study the characteristics of the vortices produced by a single pitched and skewed jet.

The early work by Wallis[1] indicated that a single vortex, similar to one from a solid generator, may be formed by a weak jet which is skewed and pitched with respect to the wall. Recently, Johnston and Nishi[3] showed that pitched and skewed jets, operated at jet speeds approximately equal to the freestream speed, produce the spanwise variation in skin friction coefficient characteristic of longitudinal vortices embedded in a turbulent boundary layer. It was concluded that longitudinal vortices were formed, but details on their strength, decay rate, and other characteristics were unknown. The single vortex formed by a skewed jet seems to be qualitatively and quantitatively different from the weaker vortex pairs that form when a jet enters a stream in crossflow through a perpendicular hole in a wall, but very little is known about generation mechanisms and the subsequent downstream development of a vortex created by a skewed jet. This paper addresses the second issue: the downstream development of such vortices.

The objective of this study was to investigate the mean velocity field downstream of a simple, round jet pitched and skewed relative to an oncoming turbulent boundary layer, in order to characterize and better understand the development of a longitudinal vortex created by the jet as it interacts with the main flow. With pitch held at 45 deg, seven cases were examined experimentally. In five cases with the skew angle set at 0, 45, 90, 135, and 180 deg to the main flow direction and the velocity ratio ($VR = U_j/U_\infty$) kept equal to 1.0, detailed mean velocity vectors were obtained across and through the region of boundary-layer/vortex interaction at four downstream stations. Also, the same kind of data were developed with the skew angle fixed at 90 deg and VR set equal to 0.7 and 1.3 in addition to $VR = 1.0$, the base case. The results are contrasted to similar results for solid vortex generators,[7–9] and the similarities and differences noted. It was clear from these data that the vortices created by the jets were structurally similar to a weak vortex formed by a solid vortex generator in addition to the similarity in stall-control effectiveness.

Methods and Conditions of the Experiment

A single 6.35-mm-diam jet was introduced through a flat test surface into a two-dimensional turbulent boundary layer. The test surface was one wall of a rectangular, constant area wind tunnel, Fig. 1, operated at freestream velocity of 15 m/s. The nozzle plug used by Nishi and Johnston (see Fig. 2 in Ref. 3) was employed here. Air was delivered to the jet with

Received Oct. 15, 1990; presented as Paper 91-0038 at the AIAA 29th Aerospace Sciences Meeting, Reno, NV, Jan. 7–10, 1991; revision received March 26, 1991; accepted for publication April 19, 1991.

*Research Assistant, Department of Mechanical Engineering.
†Professor, Department of Mechanical Engineering.

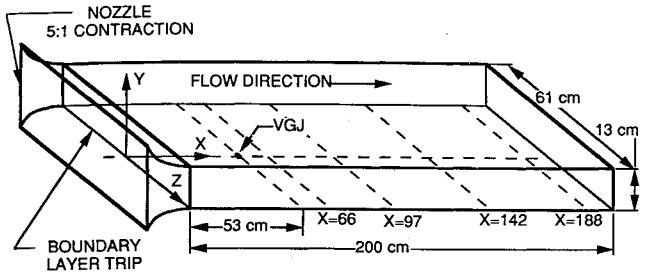

Fig. 1 Turbulent boundary-layer facility.

a small blower, and the jet speed determined by measuring Δp across the nozzle using the previously determined discharge coefficient.[3] The mass flow rate at U_j = 15 m/s was approximately 0.0005 kg/s. The point of injection was located at x = 53 cm downstream of the boundary-layer trip, and at the injection point the boundary layer's momentum thickness Reynolds number was approximately 1500 with $\delta_{99} \approx 14$ mm. The boundary layer was two-dimensional and grew slowly to a thickness of about 30 mm at the last measurement station, x = 188 cm from the trip, constituting normal growth for a two-dimensional boundary layer under a slight favorable pressure gradient.

Three components of mean velocity were obtained at four planes downstream of the jet. A five-hole pressure probe carried on a two-axis traverse system was used for these measurements. The 3.2-mm-diam five-hole probe, as described by Pauley and Eaton,[7] can measure mean velocity and pitch and yaw angles, with the mean velocity accurate within ±0.2 m/s and secondary flow angles accurate to within ±0.5 deg for flow near the wall. Pauley's data-reduction scheme and calibration constants were used. Stepper motors in the traverse system allowed z placement to within ±0.006 mm and y placement to within ±0.003 mm. For each plane of data, at least 300 points were taken across y and z at equally spaced locations on a 0.5 × 0.5 cm grid. For each of the seven cases, three kinds of basic results were obtained at each of the four data planes: 1) contours of streamwise mean velocity ratio, U/U_∞; 2) vectors at each data point to represent the secondary velocity field; and 3) contours of the secondary flow vorticity Ω_x.

Vorticity was calculated for each data point on the 0.5 × 0.5 cm grid. To obtain smooth images of vorticity contours, the velocity data were interpolated to a finer, 0.25 × 0.25 cm, mesh using natural cubic spline fits for the data. The Ω_x component of vorticity,

$$\left(\frac{\partial W}{\partial y} - \frac{\partial V}{\partial z}\right)$$

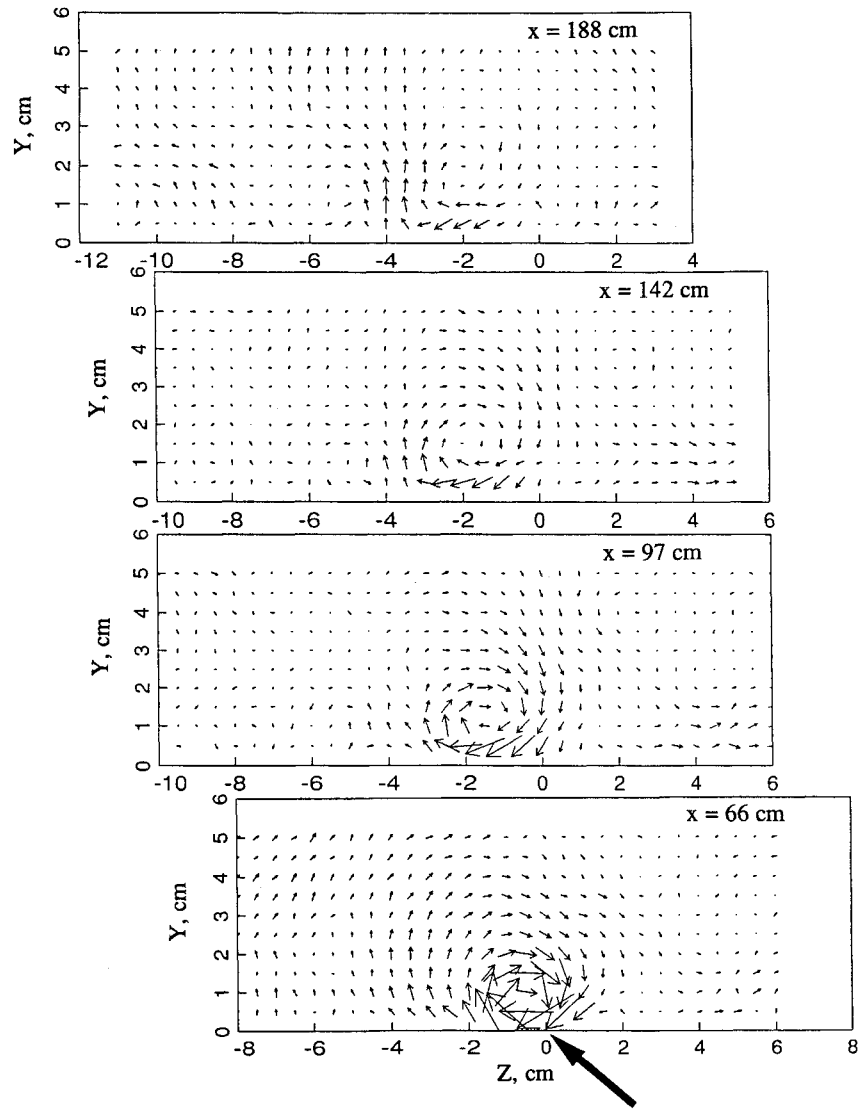

Fig. 2a Secondary velocity vectors for the case where θ = 90 deg and VR = 1.0. 1 m/s secondary velocity is indicated by a vector 2 cm long. Large arrow indicates jet orientation.

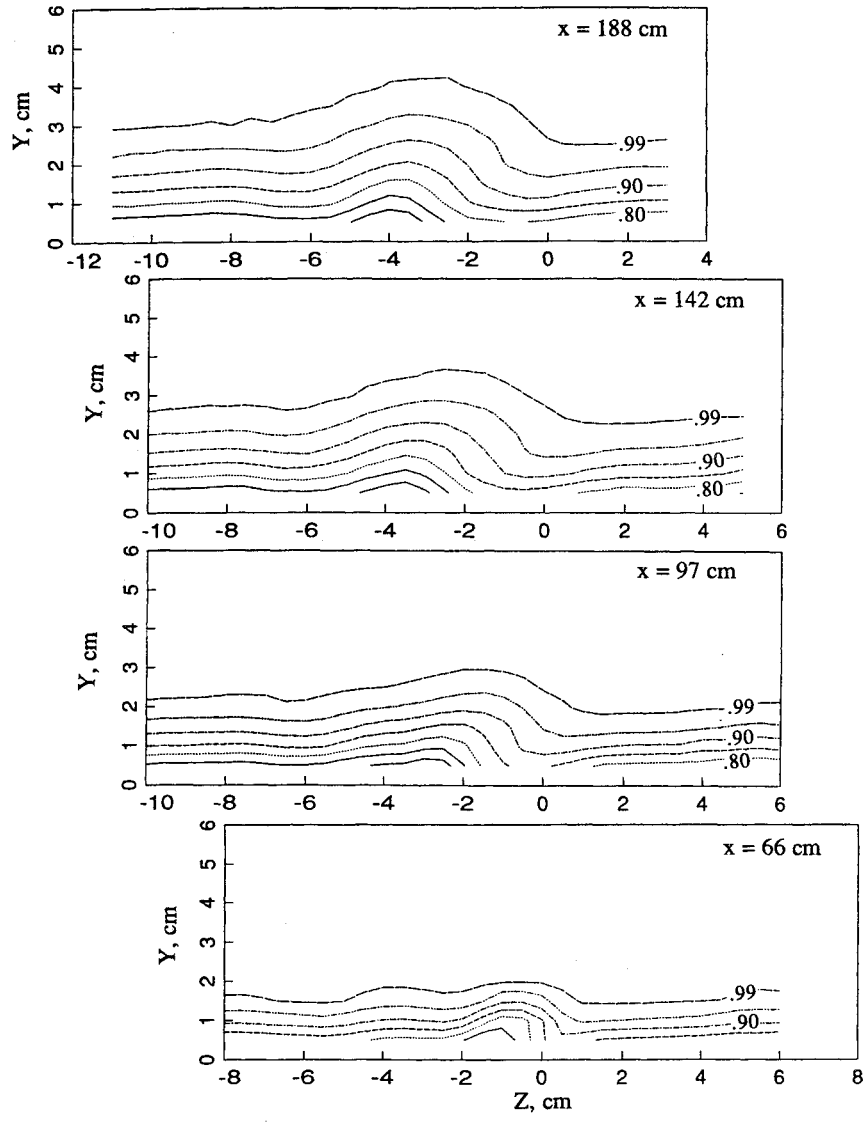

Fig. 2b U/U_∞ **contours for the case where** θ **= 90 deg and** VR **= 1.0. Intervals are by 0.05, except the final contour, which is located at** δ_{99}.

was next determined by integrating the second derivatives given by a cubic spline fit to the velocities at the more densely packed points on the fine mesh. The peak vorticity is accurate to within 7% (at most ± 40 m/s) using this method, and lower levels of vorticity are accurate to approximately ±10 m/s. Contour plots for all of the vorticity data have been generated, with the minimum contour represented 20 s^{-1} for each plot.

Circulation was then calculated for each plane of data. The contribution of disorganized low level vorticity (i.e., noise) to the circulation can be very large, so the data points that had vorticity less than a threshold level of 20 s^{-1} were ignored, while the rest were tallied to determine circulation. The positive and negative vorticities were added separately, to keep areas of strong negative vorticity from negating areas of positive vorticity. The numbers presented, therefore, are actually the sum of the positive vorticities greater than 20 s^{-1} multiplied by the area that each point represents.

Results and Discussion

The velocity profiles and vorticity contours verify the presence of longitudinal vortices generated by the jet. Detailed results are presented here for one jet configuration. For this case, the jet skew angle was 90 deg, pointing across the direction of the freestream in the negative z direction, and the jet blew at the freestream speed, VR = 1.0. Figure 2a shows the secondary velocity vectors downstream of the jet. The secondary velocity of greatest magnitude is approximately 1 m/s, or only 7% of U_∞, which makes us designate the vortex as "weak."

Although weak, the swirling motion is easily identifiable, even at the final downstream position. At successive downstream stations the core of the vortex moves in the negative z direction. At the final downstream location (188 cm) the core appears to be at $z = -2$ cm, offset by 2 cm from the jet injection location, and by 1 cm from its location at the first data station, x = 66 cm. This motion may be explained by analogy to the motion of a free potential vortex near a flat wall. The blocking effect of the wall is produced by introduction of an "image vortex" of opposite sign below the wall, and the two vortices induce a spanwise convection of the vortex cores. Viscous effects modify this concept quantitatively, but not qualitatively.

Figure 2b shows the velocity deficit contours for the same case. The thinning of the boundary layer in the downwash region of the vortex is apparent, but not very strong. This thinning of the boundary layer appears to coincide with the local enhancement of skin friction coefficient found by Nishi.[3] The contours in the downwash region at the first downstream station look quite distorted. This distortion relaxes as the vortex weakens downstream. Contour levels are not extended below y = 0.5 cm out from the wall because any attempt to use curve

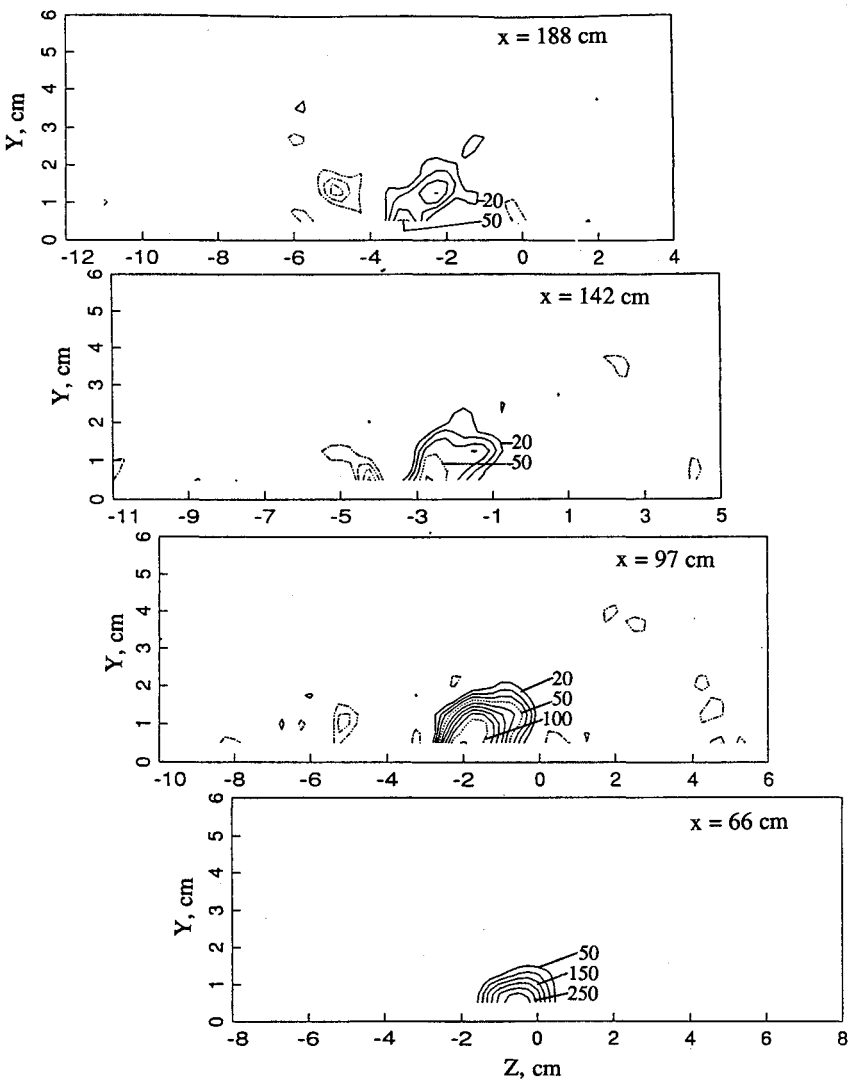

Fig. 2c Axial vorticity Ω_x for the case where θ = 90 deg and VR = 1.0. Contours are in 10 1/s levels except for x = 66 cm, where contours are multiples of 50 1/s. Lowest vorticity level shown is 20 1/s. Negative vorticity is denoted by dashes.

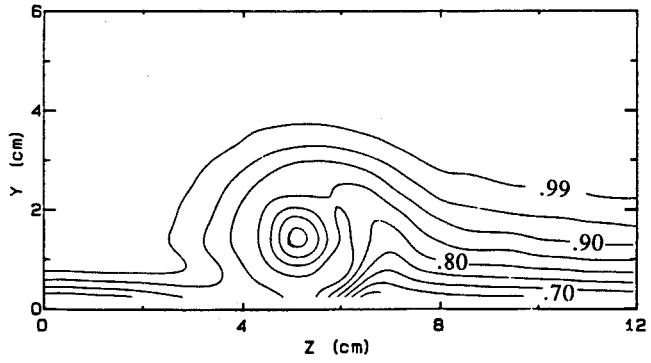

Fig. 3a U/U_∞ contours for half-delta wing of Pauley (x = 97 cm).

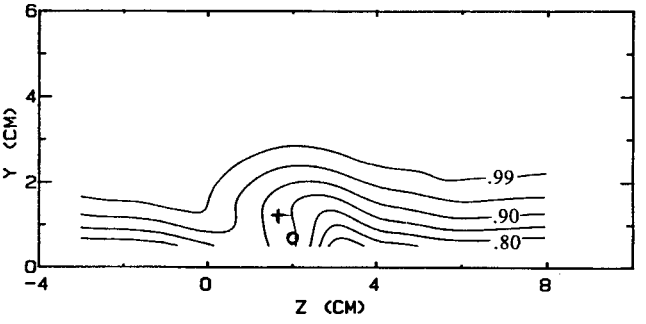

Fig. 3b U/U_∞ contours for weak vortex of Eibeck. Corresponds to x = 111 cm in current study. "+" marks center of vortex from secondary velocity vector field, and "○" denotes estimated position of maximum axial vorticity Ω_x.

fitting to extrapolate into this region would result in inaccurate boundary-layer profiles near the wall.

Figure 2c depicts the vorticity contours for these same data. It is clear that the vorticity is well organized at the first station but dissipates rapidly downstream. Contours at the first downstream station indicate vorticity as high as 300 s^{-1}. By the last station, a weak secondary vortex of opposite direction has formed near the upwash region of the primary vortex. Another characteristic of the vortex generated by all seven of the VGJ cases studied is the lack of closure of the vorticity contours. The peak in vorticity occurs at, or close to, the wall, below y = 0.5 cm, where no valid vorticity data could be obtained.

Solid vortex generator flows were studied by Pauley and Eaton[7,8] in the same facility. Similarities and differences between the vortex produced by a VGJ and a strong vortex produced by one of their solid vortex generators become evident upon examination of Fig. 3a, taken from Ref. 7. They used a half-delta generator set at 18 deg of skew, penetrating the boundary layer to about 1.5 δ_{99}. The secondary velocity pro-

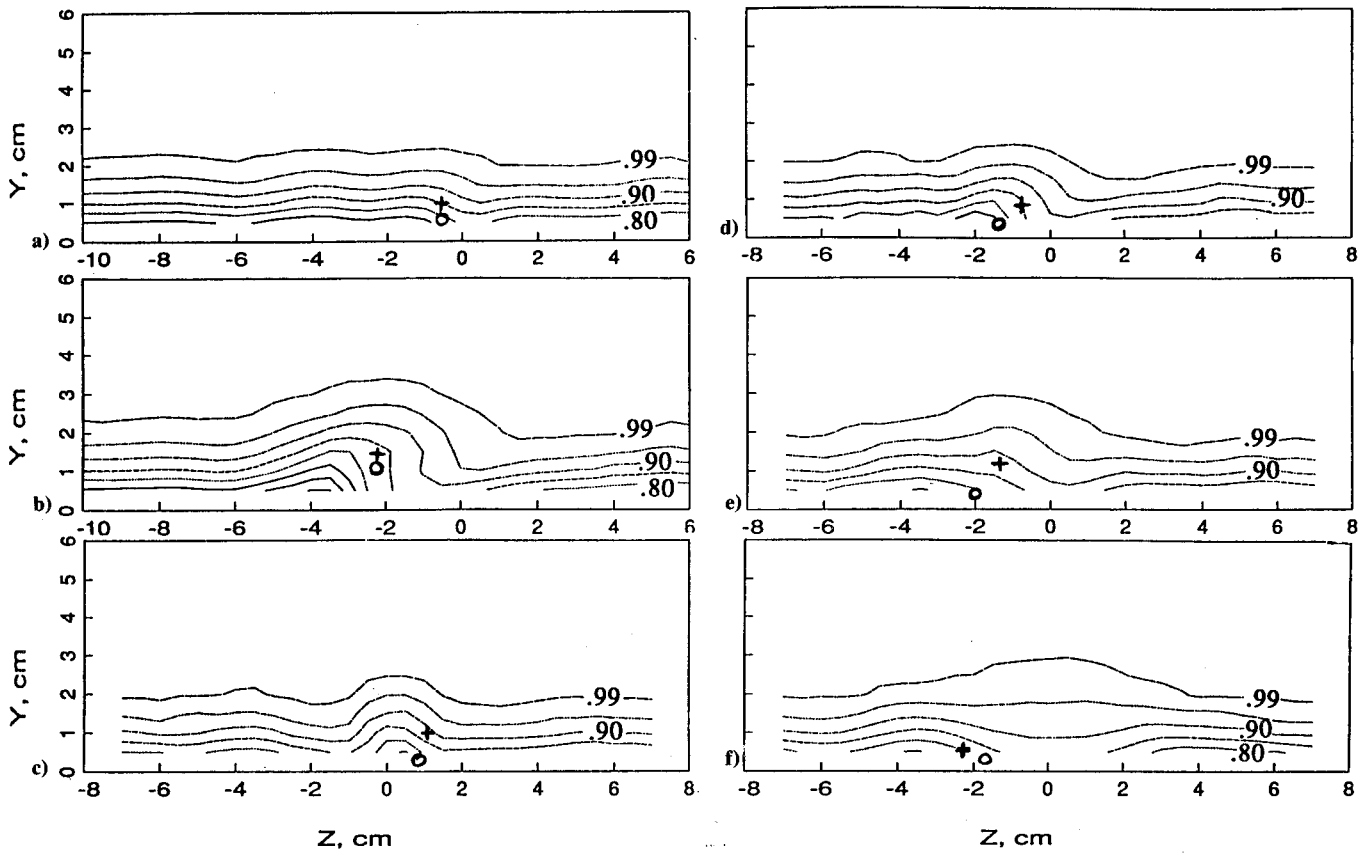

Fig. 4 U/U_∞ **contours for the six cases not shown in Fig. 2a, all at the** x **= 97 cm station. Contour intervals are by 0.05, except the final contour is at** U/U_∞ **= 0.99,** δ_{99}**. "+" marks center of vortex from secondary velocity vector field, and "○" denotes estimated position of maximum axial vorticity** Ω_x**: a)** VR **= 0.7,** θ **= 90 deg; b)** VR **= 1.3,** θ **= 90 deg; c)** VR **= 1.0,** θ **= 0 deg; d)** VR **= 1.0,** θ **= 45 deg; e)** VR **= 1.0,** θ **= 135 deg; and f)** VR **= 1.0,** θ **= 180 deg.**

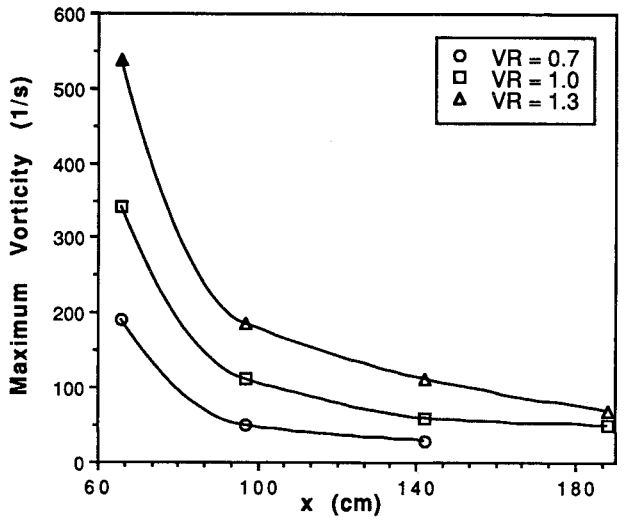

Fig. 5 Effect of jet velocity on the downstream decay of maximum positive vorticity (absolute levels; jet skew = 90 deg).

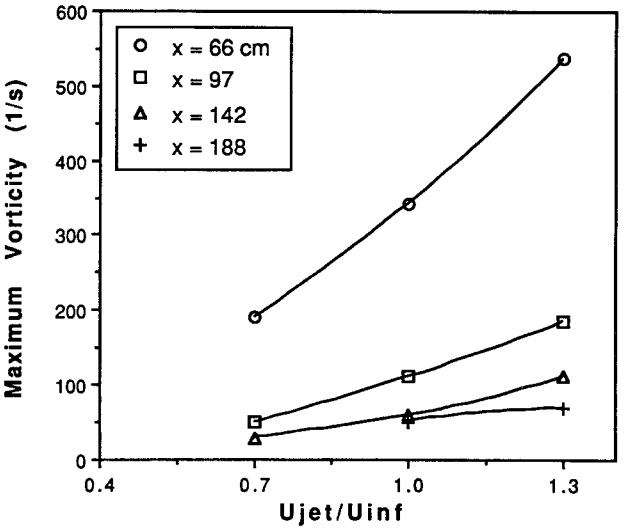

Fig. 6 Maximum positive vorticity levels as functions of jet velocity (jet skew = 90 deg).

files (not shown) are qualitatively similar, but the vortices from this solid vortex generator were substantially stronger than those from VGJs. In the velocity deficit contours, there are notable differences. First, a portion of the oncoming boundary layer was lifted up off the wall, creating a low velocity core in the center of the vortex shed downstream, but comparison of Figs. 2a and 2b shows no core of low axial velocity in the vortex generated by the VGJ. Second, the thickest part of the boundary layer does not coincide with the spanwise location of the center of the vortex for the VGJ, whereas it does for the solid vortex generator. In summary, the center of secondary circulation in the VGJ vortex does not correspond to the location of a core of minimum axial velocity, or to the location of maximum axial vorticity as is the case for the strong vortex from a solid generator.

Comparison of the VGJ flow with a weaker vortex formed by a different solid vortex generator yields more similarities. Figure 3b shows the velocity deficit contours from a study by Eibeck.[9] Again, the facility used was the same as the current study, with different downstream locations chosen for detailed

profiles. Eibeck's "Vortex II," shown here, was generated by a 1-cm-high half-delta wing (a little shorter than δ_{99}) at a 12-deg angle of attack. The velocity deficit contours do not close to form a low momentum core. Vorticity contours from her study (not shown) indicate that the location of maximum positive vorticity is closer to the wall than is the center of the swirling motion. The weaker flow from this half-delta generator looks quite similar to the flows produced by the VGJs in our study.

The six cases not presented in Fig. 2 are represented in Fig. 4, which shows the U/U_∞ contours at one x station. The vortex centers deduced from secondary velocity vector fields (not shown) and locations of maximum axial vorticity (plots not shown) are marked with "+" and "○," respectively. The location of maximum positive vorticity has been estimated based on contours that are not closed in cases c–f. Cases a and b have jet skew angle of 90 deg, with VR = 0.7 and 1.3, respectively. The stronger vortex generated by the faster jet (Fig. 4b) moves farther in the spanwise direction than do weaker vortices. The contours of Figs. 4d and 4e show that the vortices associated with the jet skewed at 45 deg and 135 deg are tighter and weaker, respectively, relative to the 90-deg jet shown in Fig. 2. In these two, the location of maximum positive vorticity is located farther along the span from the jet injection location, z = 0, than is the center of the vortex whose location is deduced from the secondary velocity field. This is different from the 90-deg jet where these two locations move about the same distance.

Special cases without skew are given in Figs. 4c and 4f. Figure 4c is the 0-deg case. The boundary layer thickens in the wake of the jet which is pointed downstream. A very weak pair of counter-rotating vortices is present here, with the common flow region between vortices flowing upward (in the positive y direction) close to z = 0. The magnitude of the largest secondary velocity in this case is approximately 3% of U_∞, compared with 7% for the base case. The "+" marks one vortex center and the "○" locates the largest positive axial vorticity. The vortex of opposite rotation and the point of peak negative vorticity are not shown here. A similar convention is used in Fig. 4f for the 180-deg case, which is also symmetric about z = 0. A weak counter-rotating vortex pair is also present, but the pair's common flow region is downward, toward the wall. The thickened region in the boundary layer is due to the wake of the main jet, but as the vortices convect downstream, they eventually thin this region (not shown).

To quantify and compare the effects of jet velocity and jet angle on rate of downstream decay, both maximum positive vorticity and positive circulation are presented in Figs. 5–11. Maximum positive vorticity was defined as the highest value

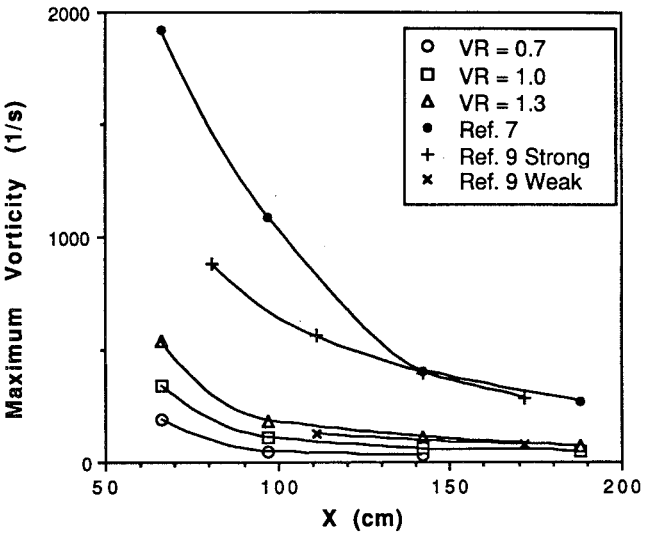

Fig. 7a Maximum positive vorticity levels, compared to solid vortex generator studies. VR varying and θ = 90 deg. Reference 9 weak case is the same as that depicted in Fig. 3b.

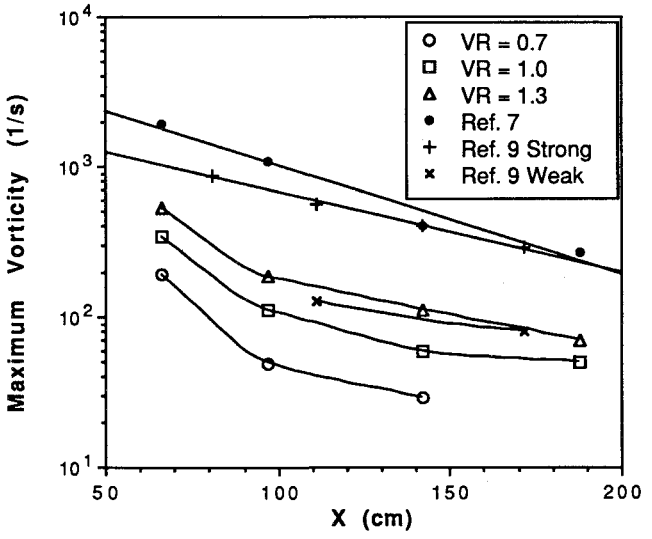

Fig. 7b Semilog representation of Fig. 7a.

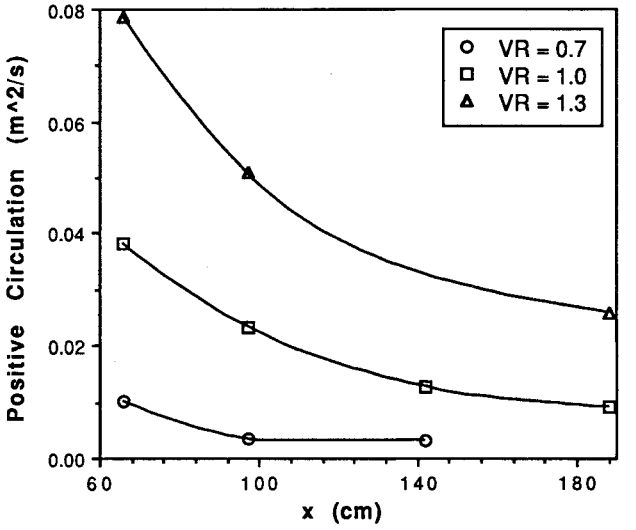

Fig. 8 Effect of jet velocity on the absolute levels of positive circulation (jet skew = 90 deg).

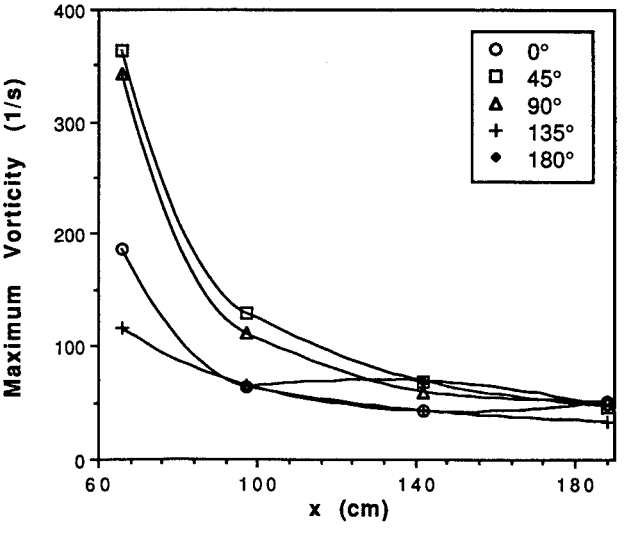

Fig. 9 Effect of jet skew angle on the downstream decay of maximum positive vorticity (absolute levels; VR = 1.0).

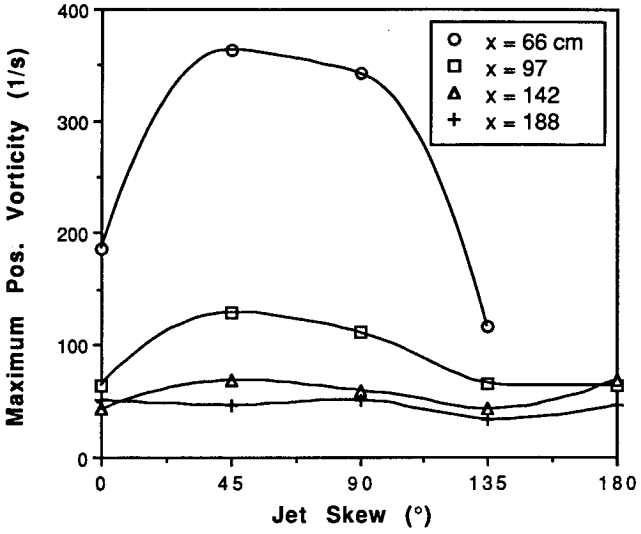

Fig. 10 Maximum positive vorticity levels as functions of jet skew angle (VR = 1.0).

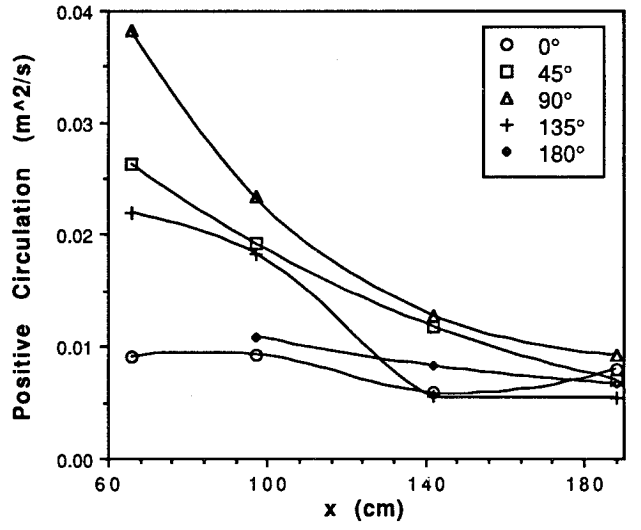

Fig. 11 Effect of jet skew angle on the absolute levels of positive circulation (VR = 1.0).

of the calculated positive vorticity at any point in each plane of data.

It is clear that the maximum vorticity is a strong function of the jet velocity as seen in Fig. 5, and the vortices generated by jets are characterized by rapid downstream decay of maximum vorticity. Looking at the maximum positive vorticity as a function of jet velocity, it appears that the maximum positive vorticity is nearly a linear function of jet velocity (see Fig. 6), but when the vorticity levels are normalized by the vorticity level at the first station for each case, it is evident that the decay rates are functionally similar. The decay rates of maximum positive vorticity from two different solid vortex generator studies[7,9] are also plotted in Fig. 7a. It shows that the jet-generated vortices decay much more rapidly at first, but more slowly further downstream, when compared with a typical strong vortex of Ref. 7. Two weaker vortices from Ref. 9 are included; the weaker of these two is the "Vortex II" depicted in Fig. 3b. Although the downstream positions are different in Ref. 9, the decay appears to be similar to that of the "base case" of Ref. 9. Figure 7b shows the same data in log-normal coordinates. From this perspective, it appears that the VGJ vortices decay more rapidly than a simple decaying exponential, while the vortices generated by half-delta wings appear to decay exponentially.

The positive circulation shown in Fig. 8 decays less rapidly than the vorticity. Decreases in circulation levels must be attributed to the spanwise shear stress diffusing the vorticity to levels below the threshold of 20 s^{-1}, below which it no longer contributes to positive circulation as defined here. Since a fairly substantial amount of circulation must exist below the area where data were taken, the circulation decay plots should be used only to indicate general trends; not for absolute values.

There is an optimal jet angle for producing maximum secondary velocities and axial vorticity. The 45-deg jet position produced a slightly higher maximum vorticity level than did the 90-deg jet position; see Fig. 9. Thus, an intermediate position—pointing slightly downstream of 90 deg—may offer the best performance in suppression of separation. Again, the maximum vorticity decays rapidly, to 30–40% of the original value at the second downstream location; Fig. 10. The decrease in positive circulation for the jet angle study is shown in Fig. 11. Compared with the 90-deg case, the 45-deg position shows a consistent small decrease in the circulation, which may be a desirable feature. The 0-deg curve actually shows a slight increase in circulation at the last station, but the levels of circulation are so small that this increase could just be an artifact of the method of calculation. The flows produced when the jet was oriented downstream at 0 deg or upstream at 180 deg were shown to produce pairs of very weak vortices. As seen in Figs. 9–11, these angular positions are likely to be of little practical interest for augmentation of boundary-layer mixing compared to cases with skew between 45 and 135 deg.

Conclusions

The current study verified that a pitched and skewed jet in a crossflow generates a longitudinal vortex.

1) The vortices produced by the jets studied were similar in many respects to a weak vortex formed by a solid vortex generator, but not to a stronger vortex from a larger generator skewed at higher angle of attack. The rate of decay of peak streamwise vorticity did not have the same near-exponential form, but the velocity deficit contours and the lack of coincidence between the location of maximum vorticity and center of swirl showed strong qualitative similarity in the case of the weaker solid generator vortex.

2) The maximum vorticity levels are strongly dependent on jet velocity and skew angle, and an optimal jet skew angle may be between 45 and 90 deg.

3) The physical mechanism for generation of a streamwise vortex by a jet is not yet understood, but the near field downstream of the jet may offer explanations for the interaction of the jet with the vorticity in the boundary layer.

Acknowledgments

The Air Force Office of Scientific Research funded this work as a portion of the Stanford "Flow Control" grant under the URI program. This paper represents a small fraction of the work supported by this multi-investigator grant. We also thank John Eaton for his assistance and equipment for this investigation.

References

[1]Wallis, R. A., "A Preliminary Note on a Modified Type of Air Jet for Boundary Layer Control," Aeronautical Research Council, Current Paper 513, London, 1960.

[2]Ball, W. H., "Tests of Wall Blowing Concepts for Diffuser Boundary Layer Control," AIAA Paper 84-1276, June 1984.

[3]Johnston, J. P., and Nishi, M., "Vortex Generator Jets—A Means for Flow Separation Control," *AIAA Journal*, Vol. 28, No. 6, 1990, pp. 989–994.

[4]Lin, J. C., Howard, F. G., Bushnell, D. M., and Selby, G. V., "Investigation of Several Passive and Active Methods for Turbulent Flow Separation Control," AIAA Paper 90-1598, Seattle, 1990.

[5]Pearcey, H. H., "Shock Induced Separation and Its Prevention," *Boundary Layer and Flow Control*, Vol. 2, Pergamon, New York, 1961, pp. 1170–1344.

[6]McManus, K. R., and Bowman, C. T., "Effects of Controlling Vortex Dynamics on the Performance of a Dump Combustor," Twenty-Third International Symposium on Combustion, Univ. d'Orleans, Orleans, France, 1990.

[7]Pauley, W. R., and Eaton, J. K., "The Fluid Dynamics and Heat Transfer Effects of Streamwise Vortices Embedded in a Turbulent Boundary Layer," Rept. MD-51, Thermosciences Div., Dept. of Mechanical Engineering, Stanford Univ., Stanford, CA, Aug. 1988.

[8]Pauley, W. R., and Eaton, J. K., "Experimental Study of the Development of Longitudinal Vortex Pairs Embedded in a Turbulent Boundary Layer," *AIAA Journal*, Vol. 26, No. 7, 1988, pp. 816–823.

[9]Eibeck, P., and Eaton, J. K., "An Experimental Investigation of the Heat Transfer Effects of a Longitudinal Vortex Embedded in a Turbulent Boundary Layer," Rept. MD-48, Thermosciences Div., Dept. of Mechanical Engineering, Stanford Univ., Stanford, CA, Nov. 1985.